

# Federated Learning of Large Models at the Edge via Principal Sub-Model Training

Yue Niu, Saurav Prakash\*

*Department of Electrical and Computer Engineering  
University of Southern California*

Souvik Kundu

*Intel AI Labs, USA*

Sunwoo Lee

*Department of Computer Engineering  
Inha University*

Salman Avestimehr

*Department of Electrical and Computer Engineering  
University of Southern California*

*yuenui, sauravpr@usc.edu*

*souvik.kundu@intel.com*

*sunwool@inha.ac.kr*

*avestime@usc.edu*

## Abstract

Limited compute and communication capabilities of edge users create a significant bottleneck for federated learning (FL) of large models. We consider a realistic, but much less explored, cross-device FL setting in which no client has the capacity to train a full large model nor is willing to share any intermediate activations with the server. To this end, we present Principal Sub-Model (PriSM) training methodology, which leverages models' low-rank structure and kernel orthogonality to train sub-models in the orthogonal kernel space. More specifically, by applying singular value decomposition (SVD) to original kernels in the server model, PriSM first obtains a set of principal orthogonal kernels in which each one is weighed by its singular value. Thereafter, PriSM utilizes our novel sampling strategy that selects different subsets of the principal kernels independently to create sub-models for clients. Importantly, a kernel with a large singular value is assigned with a high sampling probability. Thus, each sub-model is a low-rank approximation of the full large model, and all clients together achieve the near full-model training. Our extensive evaluations on multiple datasets in various resource-constrained settings show that PriSM can yield an improved performance of up to 10% compared to existing alternatives, with only around 20% sub-model training.

## 1 Introduction

Federated Learning (FL) is emerging as a popular paradigm for distributed and privacy-preserving machine learning as it allows local clients to perform ML optimization jointly without directly sharing local data McMahan et al. (2017); Kairouz et al. (2021); Li et al. (2020). Thus, it enables privacy protection on local data, and leverages distributed local training to attain a better global model. This creates opportunities for many edge devices rich in data to participate in the joint training without direct data sharing. For example, resource-limited smart home devices can train local vision or language models using private data, and achieve a server model that generalizes well to all users via federated learning Pichai (May 7, 2019).

Despite significant progress in FL in the recent past, several crucial challenges still remain when moving to the edge. In particular, limited computation and communication capacities prevent clients from learning large models for leveraging vast amounts of local data at the clients. This problem has attracted a lot of attention Diao et al. (2021); Horvath et al. (2021); Yao et al. (2021); Vepakomma et al. (2018); He et al. (2020). For example, Diao et al. (2021); Horvath et al. (2021); Yao et al. (2021) propose to assign clients with different subsets of server model depending on their available resources. However, these works have an

\*Yue Niu, Saurav Prakash equally contribute to this work.

underlying assumption that some of the clients have sufficient resources to train a nearly full large model. As a result, server model size is limited by the clients with maximum computation and communication capacities. To overcome resource constraints on clients, prior works such as Vepakomma et al. (2018); He et al. (2020) change the training paradigm by splitting a model onto server and clients. The computational burden on the clients is therefore relieved as the dominant part of the burden is offloaded to the server. However, such a methodology requires sharing of intermediate activations and/or labels with the server, which directly leaks input information and potentially compromises privacy promises of FL.

To overcome the aforementioned limitations in prior works, we focus on an even more constrained and realistic setting at the edge, in which no client is capable of training a large model nor is willing to share any intermediate data and/or labels with the server. To this end, we propose Principal Sub-Model (PriSM) training to *allow each client to only train a small sub-model, while still enabling the server model to achieve comparable accuracy as the full-model training*. We exploit low-rank structure in models during the training, which is commonly used in reducing compute costs Khodak et al. (2021); Denton et al. (2014). However, naive low-rank approximation in FL Yao et al. (2021), where all clients only train top-k kernels based on their capacities, incurs a notable accuracy drop, especially in very constrained settings. In Figure 1, we delve into this issue by showing the number of principal kernels required in the orthogonal space to accurately approximate each convolution layer in the first two *ResBlocks* in ResNet-18 He et al. (2016) during FL training<sup>1</sup>. We observe that even at the end of the FL training, around half of the principal kernels are still needed to sufficiently approximate each convolution layer. We have similar findings for the remaining convolution layers (See Sec 4.3 for results). Therefore, to avoid the reduction in server model capacity, it is essential to ensure that all server-side principal kernels are collaboratively trained on clients, especially when each client can only train a very small sub-model (e.g., <50% of the server model).

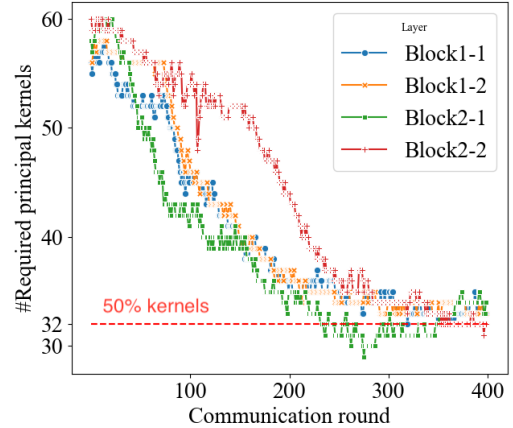


Figure 1: Number of principal kernels in the orthogonal space required to accurately approximate each of the two convolution layers in the first two ResBlocks in ResNet-18 during FL training. Block $i$ - $j$  indicates  $j$ -th convolution layer in  $i$ -th ResBlock. Each of these convolution layers has 64 kernels in the original space, which is also the maximum number of principal kernels in orthogonal space.

Based on our above observations, PriSM employs a novel probabilistic strategy to select a subset of kernels and create a sub-model for each client as shown in Figure 2. More specifically, PriSM first converts the model into orthogonal space where original convolution kernels are decomposed into principal kernels using singular value decomposition (SVD). To approximate the original server model, PriSM utilizes our novel sampling process, that is based on the singular values, such that a principal kernel with a larger singular value has a higher sampling probability. Furthermore, the probabilistic process ensures that all sub-models can together provide a near server model coverage, thus leading to the near full-model training performance.

We conduct extensive evaluations for PriSM on vision and language tasks under resourced-constrained settings where no client is capable of training the large full model. In particular, we consider both resource constraints and heterogeneity in computation, communication as well as data distribution. Our results demonstrate that PriSM delivers consistently better performance compared to other prior works, especially when participating clients have very limited capacities. For instance, on ResNet-18/CIFAR-10, we show that PriSM only incurs around 2% and 3% accuracy drop for i.i.d and highly non-i.i.d datasets under a very constrained setting where all clients can only train around 20% of the server model. Compared to other solutions, PriSM improves the accuracy by up to 10%. Furthermore, we provide detailed insights into the performance gains attained by PriSM via analysis of server model’s low-rank structure during training. In the end, we study how the sampling probability distribution in PriSM impacts the training performance.

<sup>1</sup>See Sec 4.3 for further details, especially for calculating the required number of principal kernels.

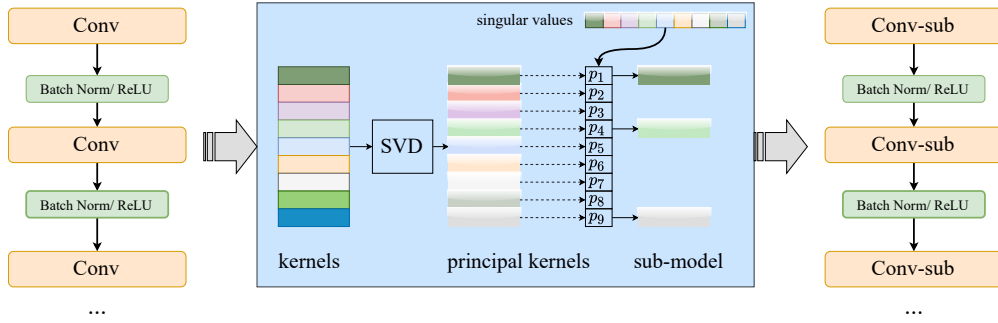


Figure 2: Creating clients’ sub-models. PriSM randomly samples a subset of principal kernels to create a client’s sub-model based on its computation and communication capacity. The sampling probability is derived from singular values of principal kernels. It ensures every sub-model approximates the full large model, and all sub-models together provide a near full server model coverage.

## 2 Related Works

**Factorized Models.** Training neural networks with layer factorization has been extensively studied in prior literature Denton et al. (2014); Khodak et al. (2021); Jaderberg et al. (2014); Novikov et al. (2015); Ioannou et al. (2016). Specifically, these works are based on the observation that well-trained neural networks have inherently low-rank structure and exhibit large-correlations across kernels. Hence, one can potentially down-size the model with a low-rank approximation to provide significant reduction in computations thus speeding up training. Furthermore, this can make model training more affordable for resource-constrained devices.

**Resource-Constrained Federated Learning.** While federated learning opens the door for collaborative model training over edge users having rich (but private) data, the computational and communication footprint prohibits training of large high-performance models at the resource-constrained clients. To address these resource limitations in federated learning, a number of works have been proposed in the literature Diao et al. (2021); Horvath et al. (2021); Yao et al. (2021); Diao et al. (2021); Horvath et al. (2021); Yao et al. (2021); Vepakomma et al. (2018); Poirot et al. (2019); Chopra et al. (2021); He et al. (2020).

The works closely related to ours are HeteroFL Diao et al. (2021), FjORD Horvath et al. (2021) and FedHM Yao et al. (2021), that aim to enable participation of a resource-constrained client by letting it train a smaller sub-model based on its capabilities. In particular, HeteroFL and FjORD create sub-models for clients by selecting certain fixed number of original kernels of the server model. On the other hand, FedHM creates sub-models using fixed subsets of factorized principal kernels. However, in these works, the size of the server model gets limited by the clients with maximum computation and communication capacities, sacrificing the model performance. This becomes even more critical in a realistic, cross-device FL setting wherein no client has the capacity to train a large model. While another work, FedPara Hyeon-Woo et al. (2021), proposes a low-rank factorized model training to reduce communication costs, computational footprint still remains prohibitive as every client is required to perform full-model training.

## 3 Method

In this section, we first motivate our proposal, Principal random Sub-Model training (PriSM), with an observation of orthogonality in convolution layers. Then, we describe the details and various aspects of PriSM.

**Notations.** We denote the Frobenius norm as  $\|\cdot\|_F$ , and  $\sigma_i$  as  $i$ -th singular value in matrix  $A$ .  $\otimes$  indicates convolution operation, and  $\cdot$  indicates simple matrix multiplication.  $\langle \cdot, \cdot \rangle$  denotes sum of element-wise multiplication or inner product.  $tr(A)$  is the trace of matrix  $A$ .

### 3.1 Motivation: An Observation on Orthogonality

We consider a convolution layer with kernels  $W \in \mathbb{R}^{N \times M \times k \times k}$  and input  $X \in \mathbb{R}^{M \times H \times W}$ , where  $N$  and  $M$  respectively denote the number of output channels and the number of input channels,  $k$  is kernel size, and  $H \times W$  is the size of the input image along each channel. Based on a commonly used technique *im2col* Chellapilla et al. (2006), the convolution layer can be converted to matrix multiplication as  $\bar{Y} = \bar{W} \cdot \bar{X}$ , where  $\bar{W} \in \mathbb{R}^{N \times Mk^2}$  and  $\bar{X} \in \mathbb{R}^{Mk^2 \times HW}$ . For kernel decorrelation, we apply singular value decomposition (SVD) to map kernels into orthogonal space as:  $\bar{W} = \sum_{i=1}^N \sigma_i \cdot \mathbf{u}_i \cdot \mathbf{v}_i^T$ , where  $\{\mathbf{u}_i\}_{i=1}^N, \{\mathbf{v}_i\}_{i=1}^N$  are two sets of orthogonal vectors<sup>2</sup>. The convolution can be decomposed as follows:

$$\bar{Y} = \sum_{i=1}^N \bar{Y}_i = \sum_{i=1}^N \sigma_i \cdot \mathbf{u}_i \cdot \mathbf{v}_i^T \cdot \bar{X}. \quad (1)$$

For  $\forall i \neq j$ , it is easy to verify that  $\langle \bar{Y}_i, \bar{Y}_j \rangle = \sigma_i \cdot \sigma_j \cdot \text{tr}(\bar{X}^T \cdot \mathbf{v}_i \cdot \mathbf{u}_i^T \cdot \mathbf{u}_j \cdot \mathbf{v}_j^T \cdot \bar{X}) = 0$ , namely the output features  $\bar{Y}_i$  and  $\bar{Y}_j$  are orthogonal. Therefore, if we regard  $\bar{W}_i = \sigma_i \cdot \mathbf{u}_i \cdot \mathbf{v}_i^T$  as a principal kernel, different principal kernels create orthogonal output features. To illustrate this, Figure 3 shows a input image (left) and the outputs (right three) generated by principal kernels. We can observe that principal kernels captures different features and serve different purposes.

As Xie et al. (2017); Balestrierio et al. (2018); Wang et al. (2020) reveal, imposing orthogonality on kernels leads to better training performance. This motivates us to initiate the training with a set of orthogonal kernels. Furthermore, to preserve kernel orthogonality during training, it is critical to constantly refresh the orthogonal space through re-decomposition. The above intuitions based on the observation on orthogonality play an important role in PriSM, which is described in the following section.

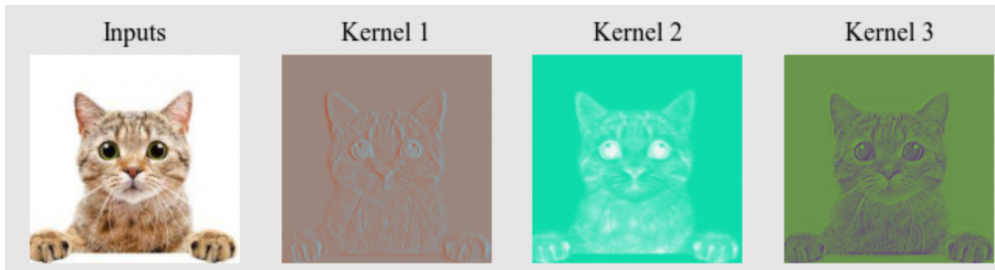


Figure 3: Orthogonal outputs generated by principal kernels  $\bar{W}_i$ . Different principal kernels capture different features: Kernel 1 extracts the outline of an object, Kernel 2 and 3 capture detailed textures of the object but on distinct regions.

**Remark 3.1.** *The layer decomposition using SVD also applies to fully-connected and LSTM layers, where weights  $W \in \mathbb{R}^{N \times M}$ . we can directly apply SVD and obtain the principal components.*

### 3.2 PriSM: Principal Random Sub-Model Training

In the realistic setting considered in our paper, participating clients are very resource-limited and incapable of performing full large model training. Therefore, to train a large server model in FL, it is essential to distribute the training workloads among clients. One way to achieve this goal is to select a subset of the server model and assign to clients. Based on the motivation in Section 3.1 to train orthogonal kernels, we select sub-models and sample from the orthogonal space. Further, as we observe in Section 3.1, different principal kernels capture distinct features in the orthogonal space, and their contributions are further weighed by their corresponding singular values as shown in Eq. (1). Therefore, we propose a novel importance-aware sampling strategy to create sub-models for clients. This provides two key benefits: 1) each sub-model is a low-rank approximation to the server model; 2) the conglomerate of the sampled sub-models enables a near-full server model coverage. Each participating client trains its sub-model and uploads it to the server.

<sup>2</sup>We assume WLOG  $\bar{W}$  is a tall matrix.

The server then aggregates the updated sub-models, obtain the full model in the original space, and then re-decompose it to refresh the orthogonal space for the next communication round.

---

**Algorithm 1** PriSM: Principal Random Sub-Model Training

---

**Input:** layer parameters  $W$ , client capacities.

```

1: for communication round  $t = 1, \dots, T$  do
2:   Decompose  $W$  into orthogonal kernel using SVD  $\rightarrow \{\overline{W}_i\}_{i=1}^N$ .
3:   Choose a subset of clients  $\rightarrow \mathcal{C}$ .
4:   for each client  $c \in \mathcal{C}$  do
5:     // Sub-model sampling
6:     Compute the sub-model size for client  $c \rightarrow |\mathcal{I}_c|$ .
7:     Obtain a sub-model using random sampling based on Eq. (2)  $\rightarrow \mathcal{I}_c, \overline{W}^c$ .
8:     // Local training
9:     Perform LocalTrain  $\leftrightarrow \mathcal{I}_c, \overline{W}^c$ .
10:  end for
11:  Aggregate parameters based on Eq. (3)  $\overline{W} \leftarrow \left\{ \overline{W}^c \right\}_{c \in \mathcal{C}}$ . // Sub-model aggregation
12:  Reconstruct  $W$  from  $\overline{W}$ . // Orthogonal space refresh
13: end for

|-----
14: LocalTrain  $\leftrightarrow \mathcal{I}_c, \overline{W}^c$ 
15: for local iteration  $k = 1, \dots, K$  do
16:   Sample an input batch from the local dataset  $\rightarrow \mathcal{D}_k$ .
17:   Perform the forward and backward pass  $\leftarrow \mathcal{D}_k, \overline{W}^c$ .
18:   Compute additional gradients from regularization based on Eq. (4)  $\leftarrow reg$ .
19:   Update the local sub-model using SGD  $\rightarrow \overline{W}^c$ .
20: end for
|-----

```

---

We describe each components of PriSM below.

**Sub-model sampling.** Given a resource budget in the client, suppose it can at most process  $r$  principal kernels for a convolution layer. For a convolution layer with principal kernels  $\{\overline{W}_i\}_{i=1}^N$ , and the corresponding singular values  $\{\sigma_i\}_{i=1}^N$ , we randomly sample  $r$  principal kernels denoted by  $\mathcal{I}_c$  without replacement with sampling probability for  $i$ -th kernel as follows:

$$p_i = \frac{\sigma_i^\kappa}{\sum_{j=1}^N \sigma_j^\kappa}. \quad (2)$$

Here,  $\kappa$  in Eq. (2) is a smooth factor that controls the probability distribution for principal kernels to be chosen. Therefore, with our proposed stochastic sampling strategy, *important* kernels with large singular values are more likely to be chosen, and all sub-models together provide a near-full model coverage. The resulting sub-model hence has smaller convolution layers. Other element-wise layers such as ReLU and batch normalization remain the same.

**Local training.** On each client, when performing optimization, the selected  $\{\mathbf{u}_i, \mathbf{v}_i\}_{i \in \mathcal{I}_c}$  are optimized, together with trainable parameters in other layers. While in PriSM, singular values  $\{\sigma_i\}_{i \in \mathcal{I}_c}$  are not updated during local training. This is because each singular value indicates *importance* of each principal kernel. Thus, freezing singular values across clients helps maintain consistency regarding importance for kernels and is useful in the aggregation of the sub-models as described next.

**Sub-model aggregation.** On the server side, with sub-models obtained from clients, we first aggregate  $i$ -th principal kernel as follows:

$$\bar{W}_i = \sigma_i \cdot \left( \sum_{c \in \mathcal{C}} \alpha_i^c \mathbf{u}_i^c \right) \cdot \left( \sum_{c \in \mathcal{C}} \alpha_i^c \mathbf{v}_i^c \right)^T, \quad (3)$$

where  $\mathcal{C}$  denotes the subset of active clients,  $\alpha_i$  is the aggregation coefficient for  $i$ -th kernel. We propose a weighted averaging scheme: if  $i$ -th kernel is selected and trained by  $C_i$  clients, then  $\alpha_i^c = 1/C_i$ . Furthermore, for principal kernels that are not sampled during creation of sub-models, they remain intact during aggregation.

**Orthogonal space refresh.** The full model in the original space is constructed by converting each 2-dimensional  $\bar{W}_i$  to the original dimension  $\mathbb{R}^{M \times k \times k}$  and combining them. For the next communication round, the orthogonal space is refreshed by decomposing the updated  $\bar{W}$  using SVD.

We further use two additional techniques to improve learning efficiency in the orthogonal space: activation normalization, and regularization on orthogonal kernels.

**Activation normalization.** We apply batch normalization without tracking running statistics; namely, the normalization always uses current batch statistics in the training and evaluation phases. Each client applies normalization separately with no sharing of statistics during model aggregation. Such an adaptation is effective in ensuring consistent outputs between different sub-models and avoids potential privacy leakage through the running statistics Andreux et al. (2020). Hence, it has been used in several sub-model FL training schemes Diao et al. (2021); Yao et al. (2021).

**Regularization.** When learning a sampled subset of principal kernels on a client, naively applying weight decay to  $\mathbf{u}_i$  and  $\mathbf{v}_i$  separately results in poor final accuracy. Inspired by Khodak et al. (2020), for training on client  $c$ , we add regularization to the subset of kernels as follows:

$$reg = \frac{\lambda}{2} \left\| \sum_{i \in \mathcal{I}_c} \sigma_i \cdot \mathbf{u}_i \cdot \mathbf{v}_i^T \right\|_F^2, \quad (4)$$

where  $\lambda$  is the regularization factor,  $\mathcal{I}_c$  denotes the subset of principal kernels on client  $c$ .

Algorithm 1 presents an overall description of PriSM. We only show the procedure on a single convolution layer with kernels  $W$  for the sake of simplifying notations.

In the following remarks, we differentiate PriSM from Dropout and Low-Rank compression.

**Remark 3.2. PriSM vs Dropout.** *Sampling a subset of kernels in PriSM shares some computation similarity with full model training using regular dropout Tompson et al. (2015) in clients. However, regular dropout on the original kernels leads to significant convergence instability due to inconsistent activations across iterations, especially with a high dropout probability Horvath et al. (2021). In contrast, PriSM performs importance-aware sampling in the orthogonal space based on singular values. Therefore, each sub-model is an approximation to the full model, and training different sub-models on different clients does not create significant inconsistency.*

**Remark 3.3. PriSM vs Low-Rank Compression.** *While PriSM exploits low-rank properties in models, it is not a low-rank compression method. Low-rank compression methods aim to construct a smaller server model by completely discarding some kernels even though they can still contribute to training performance (See Figure 5 in Section 4.3). PriSM randomly select sub-models so that every kernel is possible to be learned.*

## 4 Experiments

We evaluate PriSM under resourced-constrained settings where no clients are capable of training the large full model. Furthermore, we consider both homogeneous and heterogeneous client settings. Specifically, in homogeneous settings, all clients have the same limited compute and communication capacity, while in heterogeneous settings, clients' capacities might vary. We also compare PriSM with two other baselines: ordered kernel dropout in orthogonal space (OrthDrop), such as in Yao et al. (2021); and ordered kernel dropout in original space (OrigDrop), such as in Horvath et al. (2021); Diao et al. (2021). Additionally, we

provide more insights into the superior performance of PriSM by analyzing server model’s low-rank structure during training.

**Models and Datasets.** We train ResNet-18 on CIFAR-10 Krizhevsky et al. (2009), CNN on FEMNIST Caldas et al. (2018) and LSTM model on IMDB Maas et al. (2011)<sup>3</sup>. ResNet-18 is optimized for CIFAR-10, where kernel size in the first convolution layer is reduced to  $3 \times 3$ . CNN is a small model with two convolution layers. Detailed architectures are provided in Appendix A.1.

**Data Distribution.** For CIFAR-10 and IMDB, we create balanced datasets during training with FL. Given the total number of samples and participating clients, we uniformly sample the equal number of training images for each client when creating i.i.d datasets. For non-i.i.d datasets, we first use Dirichlet function  $\text{Dir}(\alpha)$  Reddi et al. (2020) to create sampling probability for each client and then sample an equal number of training images for clients. We create two different non-i.i.d datasets with  $\alpha = 1$  and  $\alpha = 0.1$ , where a smaller  $\alpha$  denotes a higher degree of non-i.i.d. For FEMNIST Caldas et al. (2018), we directly use the dataset without any additional preprocessing.

**FL Setting.** We simulate an FL setting with 100 clients, and 20 clients are chosen uniformly at random in each communication round. Each client trains its model for 2 local epochs and then uploads it to the aggregation server. We use SGD with momentum in the local training. The learning rate is initially 0.1 for ResNet-18/CIFAR-10 and 0.01 for CNN/FEMNIST, and is decayed by a cosine annealing scheduler. Further details are provided in Appendix A.2.

#### 4.1 Performance on Homogeneous Clients

In this setting, we assume that all clients have the same limited compute and communication capacity. We vary the client sub-model size from 0.2 to 0.8 of the full server model, where  $0.\times$  indicates only a  $0.\times$  subset of the principal kernels are sampled in each convolution layer from the server model (denoted as *keep ratio* in the results). In Table 1, we list the computational and communication footprints for different sub-models of ResNet-18. For OrthDrop, we follow the strategy in Yao et al. (2021) and select the top  $0.\times$  principal kernels for all clients. For OrigDrop, we select the first  $0.\times$  original kernels as in Diao et al. (2021); Horvath et al. (2021).

Table 1: Model size and compute costs for different sub-models in PriSM.

Model fraction	Full	0.8	0.6	0.4	0.2
ResNet-18 on CIFAR-10					
Params	11 M	9.9 M (90%)	7.4 M (67%)	4.9 M (44%)	2.5 M (22%)
MACs	1.1 G	0.9 G (80%)	0.7 G (60%)	0.5 G (45%)	0.25 G (22%)

Figure 4 shows final validation accuracy of ResNet-18 with different sampled sub-model sizes on i.i.d and non-i.i.d ( $\alpha = 1, 0.1$ ) local datasets. We note that PriSM constantly delivers better performance than the other two baselines. The performance gap is even more striking under very constrained settings. For instance, when only  $0.2\times$  sub-models are supported on clients, PriSM attains comparable accuracy as full-model training, and achieves up to 10% performance improvement compared to OrthDrop on non-i.i.d dataset with  $\alpha = 0.1$ . Furthermore, we make two key observations. First, training with sub-models in the orthogonal space (OrthDrop) provides better performance than in the original space (OrigDrop), which aligns with our intuition in Section 3.1. Second, our importance-aware sampling strategy for creating sub-models is indispensable as demonstrated by the notable performance gap between PriSM and OrthDrop.

#### 4.2 Performance on Heterogeneous Clients

To simulate clients with varying limited capacity, we simulate the following two settings: 1) 40% clients can train 0.4 sub-models, and 60% clients can only train 0.2 sub-models; 2) 20% clients can train 0.6 sub-models,

<sup>3</sup>Due to the page limit, LSTM results are deferred to Appendix A.

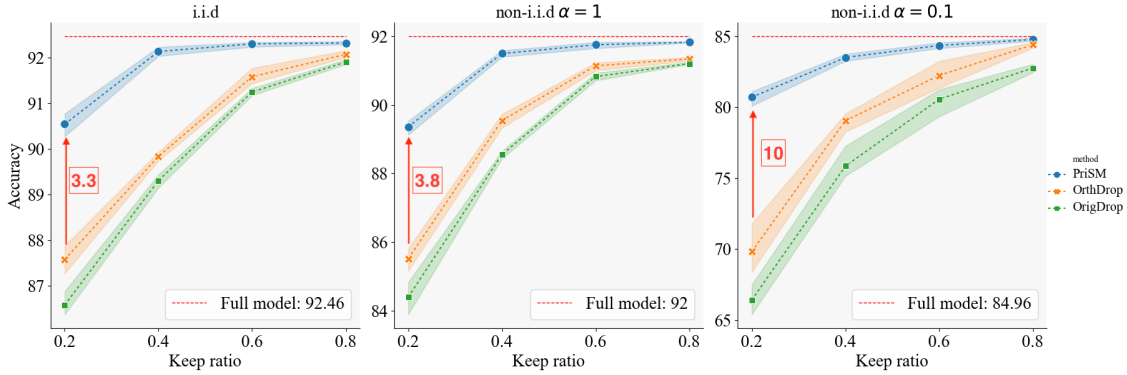


Figure 4: Training performance on CIFAR-10 on homogeneous clients. PriSM constantly delivers better performance compared to prior baselines, especially under very constrained settings.

30% clients can train 0.4 sub-models and 50% clients can only train 0.2 sub-models. No participating client trains the full model. For baseline methods, we follow the same strategy to select kernels as in Section 4.1.

Table 2: Training performance of ResNet-18/CIFAR-10 on heterogeneous clients.

Data Distribution	Baseline	Setting 1 (0.4-0.2)			Setting 2 (0.6-0.4-0.2)		
		OrigDrop	OrthDrop	PriSM	OrigDrop	OrthDrop	PriSM
i.i.d	92.46	88.86	89.57	91	88.04	90.98	91.35
non-i.i.d (1)	92	86.91	88.78	90	87.25	90.39	90.57
non-i.i.d (0.1)	84.96	76.38	78.37	80.86	80.35	81.76	81.95

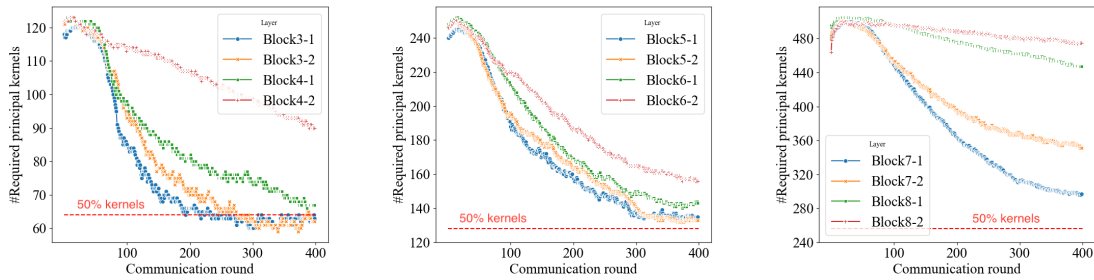
Table 2 lists the final accuracy achieved by different methods under these two settings. In Setting 2, where strong clients that support  $0.6\times$  sub-models are involved, the performance gap between PriSM and baseline methods is shrunk. However, PriSM greatly outperforms the baseline methods in the very constrained Setting 1, where only up to  $0.4\times$  sub-models are supported on a small fraction of clients. Furthermore, similar to the results in Section 4.1, the benefits of training in the orthogonal space and importance-aware sampling strategy are also observed in heterogeneous client settings.

### 4.3 Insights into PriSM: Model’s Rank during Training

Having demonstrated the performance gains of PriSM over the prior works, we now focus on providing further insights into PriSM by analyzing some of its key aspects. To this end, we first examine the low-rank structure of models during training, and pinpoint the cause behind the accuracy gap between fixed and random kernel dropout strategies in the orthogonal space.

To analyze the server model’s low-rank structure, we adopt a similar method as in Alter et al. (2000) to calculate the required number of principal kernels to accurately approximate each layer as  $2^{-\log(\sum_i p_i \log p_i)}$ . Here,  $p_i$  is calculated as in Eq. (2) with  $\kappa = 2$ . Figure 5 shows the number of kernels required to approximate each layer with  $3\times 3$  kernels in ResNet-18 during FL with full models, where Block  $i-j$  indicates  $j$ -th convolution layer in  $i$ -th ResBlock. First, we observe that while the server model attains a low-rank structure during training, a randomly initialized model does not exhibit a low-rank structure. Therefore, selecting a fixed set of top- $k$  principal kernels for the sub-models inevitably causes reductions in the server model capacity. Furthermore, even at the end of the FL training, around half principal kernels are still required to approximate most layers. In fact, some layers require even more principal kernels. Therefore, our probabilistic sampling scheme is essential in preserving the server model capacity during FL training with sub-models.





(a) ResBlock 3, 4 (128 kernels). (b) ResBlock 5, 6 (256 kernels). (c) ResBlock 7, 8 (512 kernels).

Figure 5: The number of principal kernels required to accurately approximate each convolution layer in ResBlocks 3-8 in ResNet-18 (Results of ResBlocks 1 and 2 are discussed in Figure 1).

## 5 Conclusion

We have considered the practical, yet under-explored, problem of federated learning in a resource-constrained edge setting, where no participating client has the capacity to train a large model. As our main contribution, we propose the PriSM training methodology, that empowers the resource-limited clients by enabling them to train smaller sub-models. At the same time, PriSM utilizes a novel sampling approach to obtain sub-models for the clients, all of which together ensure that the server model achieves close to the full-model performance. Our extensive empirical results demonstrate that PriSM performs significantly better than the prior baselines, especially when each client can train only a very small sub-model. In particular, when each client is required to train a sub-model that is only around 20% in size of the server model, we demonstrate that PriSM achieves a performance advantage of up to 10% over the prior baselines. While this work demonstrate the promises of importance-aware sampling strategy in improving training performance, it can be further optimized to more effectively provide near full model coverage during FL training.

## References

- Orly Alter, Patrick O Brown, and David Botstein. Singular value decomposition for genome-wide expression data processing and modeling. *Proceedings of the National Academy of Sciences*, 97(18):10101–10106, 2000.
- Mathieu Andreux, Jean Ogier du Terrail, Constance Beguier, and Eric W Tramel. Siloed federated learning for multi-centric histopathology datasets. In *Domain Adaptation and Representation Transfer, and Distributed and Collaborative Learning*, pp. 129–139. Springer, 2020.
- Randall Balestriero et al. A spline theory of deep learning. In *International Conference on Machine Learning*, pp. 374–383. PMLR, 2018.
- Sebastian Caldas, Sai Meher Karthik Duddu, Peter Wu, Tian Li, Jakub Konečný, H Brendan McMahan, Virginia Smith, and Ameet Talwalkar. Leaf: A benchmark for federated settings. *arXiv preprint arXiv:1812.01097*, 2018.
- Kumar Chellapilla, Sidd Puri, and Patrice Simard. High performance convolutional neural networks for document processing. In *Tenth international workshop on frontiers in handwriting recognition*. Suvisoft, 2006.
- Ayush Chopra, Surya Kant Sahu, Abhishek Singh, Abhinav Java, Praneeth Vepakomma, Vivek Sharma, and Ramesh Raskar. Adasplit: Adaptive trade-offs for resource-constrained distributed deep learning. *arXiv preprint arXiv:2112.01637*, 2021.
- Emily L Denton, Wojciech Zaremba, Joan Bruna, Yann LeCun, and Rob Fergus. Exploiting linear structure within convolutional networks for efficient evaluation. *Advances in neural information processing systems*, 27, 2014.

- 
- Enmao Diao, Jie Ding, and Vahid Tarokh. HeteroFL: Computation and communication efficient federated learning for heterogeneous clients. *International Conference on Learning Representations*, 2021.
- Chaoyang He, Murali Annavaram, and Salman Avestimehr. Group knowledge transfer: Federated learning of large CNNs at the edge. *Advances in Neural Information Processing Systems*, 33:14068–14080, 2020.
- Kaiming He, Xiangyu Zhang, Shaoqing Ren, and Jian Sun. Deep residual learning for image recognition. In *Proceedings of the IEEE conference on computer vision and pattern recognition*, pp. 770–778, 2016.
- Samuel Horvath, Stefanos Laskaridis, Mario Almeida, Ilias Leontiadis, Stylianos Venieris, and Nicholas Lane. FjORD: Fair and accurate federated learning under heterogeneous targets with ordered dropout. *Advances in Neural Information Processing Systems*, 34, 2021.
- Nam Hyeon-Woo, Moon Ye-Bin, and Tae-Hyun Oh. Fedpara: Low-rank hadamard product for communication-efficient federated learning. *arXiv preprint arXiv:2108.06098*, 2021.
- Yani Ioannou, Duncan Robertson, Jamie Shotton, Roberto Cipolla, and Antonio Criminisi. Training CNNs with low-rank filters for efficient image classification. *International Conference on Learning Representations (ICLR)*, 2016.
- Max Jaderberg, Andrea Vedaldi, and Andrew Zisserman. Speeding up convolutional neural networks with low rank expansions. *British Machine Vision Conference (BMVC)*, 2014.
- Peter Kairouz, H Brendan McMahan, Brendan Avent, Aurélien Bellet, Mehdi Bennis, Arjun Nitin Bhagoji, Kallista Bonawitz, Zachary Charles, Graham Cormode, Rachel Cummings, et al. Advances and open problems in federated learning. *Foundations and Trends® in Machine Learning*, 14(1–2):1–210, 2021.
- Mikhail Khodak, Neil A Tenenholz, Lester Mackey, and Nicolo Fusi. Initialization and regularization of factorized neural layers. In *International Conference on Learning Representations*, 2020.
- Mikhail Khodak, Neil Tenenholz, Lester Mackey, and Nicolo Fusi. Initialization and regularization of factorized neural layers. *International Conference on Learning Representations (ICLR)*, 2021.
- Alex Krizhevsky, Geoffrey Hinton, et al. Learning multiple layers of features from tiny images. 2009.
- Tian Li, Anit Kumar Sahu, Ameet Talwalkar, and Virginia Smith. Federated learning: Challenges, methods, and future directions. *IEEE Signal Processing Magazine*, 37(3):50–60, 2020.
- Andrew Maas, Raymond E Daly, Peter T Pham, Dan Huang, Andrew Y Ng, and Christopher Potts. Learning word vectors for sentiment analysis. In *Proceedings of the 49th annual meeting of the association for computational linguistics: Human language technologies*, pp. 142–150, 2011.
- Brendan McMahan, Eider Moore, Daniel Ramage, Seth Hampson, and Blaise Aguera y Arcas. Communication-efficient learning of deep networks from decentralized data. In *Artificial intelligence and statistics*, pp. 1273–1282. PMLR, 2017.
- Alexander Novikov, Dmitrii Podoprikin, Anton Osokin, and Dmitry P Vetrov. Tensorizing neural networks. *Advances in neural information processing systems*, 28, 2015.
- Sundar Pichai. Google’s Sundar Pichai: Privacy Should Not Be a Luxury Good. In *New York Times*, May 7, 2019.
- Maarten G Poirot, Praneeth Vepakomma, Ken Chang, Jayashree Kalpathy-Cramer, Rajiv Gupta, and Ramesh Raskar. Split learning for collaborative deep learning in healthcare. *arXiv preprint arXiv:1912.12115*, 2019.
- Sashank Reddi, Zachary Charles, Manzil Zaheer, Zachary Garrett, Keith Rush, Jakub Konečný, Sanjiv Kumar, and H Brendan McMahan. Adaptive federated optimization. *arXiv preprint arXiv:2003.00295*, 2020.

---

Jonathan Tompson, Ross Goroshin, Arjun Jain, Yann LeCun, and Christoph Bregler. Efficient object localization using convolutional networks. In *Proceedings of the IEEE conference on computer vision and pattern recognition*, pp. 648–656, 2015.

Praneeth Vepakomma, Otkrist Gupta, Tristan Swedish, and Ramesh Raskar. Split learning for health: Distributed deep learning without sharing raw patient data. *arXiv preprint arXiv:1812.00564*, 2018.

Jiayun Wang, Yubei Chen, Rudrasis Chakraborty, and Stella X Yu. Orthogonal convolutional neural networks. In *Proceedings of the IEEE/CVF conference on computer vision and pattern recognition*, pp. 11505–11515, 2020.

Di Xie, Jiang Xiong, and Shiliang Pu. All you need is beyond a good init: Exploring better solution for training extremely deep convolutional neural networks with orthonormality and modulation. In *Proceedings of the IEEE Conference on Computer Vision and Pattern Recognition*, pp. 6176–6185, 2017.

Dezhong Yao, Wanning Pan, Yao Wan, Hai Jin, and Lichao Sun. FedHM: Efficient Federated Learning for Heterogeneous Models via Low-rank Factorization. *arXiv preprint arXiv:2111.14655*, 2021.

## A Appendix

## B Appendix

### B.1 Models and Hyperparameters

In this section, we provide detailed information about models and hyperparameter settings for the results presented in the paper. We will open our source code upon acceptance of the paper.

#### B.1.1 Models

**ResNet-18/CIFAR-10.** We use a ResNet-18 optimized for CIFAR-10, in which kernel size in the first convolution layer is changed from  $7 \times 7$  to  $3 \times 3$ . Details are shown in Table 3.

#### B.1.2 Training Hyperparameters

**ResNet-18/CIFAR-10 on homogeneous clients.** We simulate 100 clients during FL training, in which each client is assigned 500 training samples for both i.i.d and non-i.i.d datasets. In each communication round, each client performs local training for 2 epochs using the local data, then uploads parameters to the server for aggregation. Table 4 lists detailed hyperparameters during FL training with ResNet-18.

**ResNet-18/CIFAR-10 on heterogeneous clients.** We adopt the same setting as in Table 4, except the fact that clients might vary in computation and communication capacity. Therefore different model might train sub-models with different sizes (See Sec 4.2 in the main paper).

Table 3: ResNet-18/CIFAR-10

Module		#kernels	size	stride	Batch Norm	ReLU	Downsample
Conv1		64	3	1	✓	✓	✗
ResBlock 1	Block1-1	64	3	1	✓	✓	✗
	Block1-2	64	3	1	✓	✓	✗
ResBlock 2	Block2-1	64	3	1	✓	✓	✗
	Block2-2	64	3	1	✓	✓	✗
ResBlock 3	Block3-1	128	3	1	✓	✓	✓
	Block3-2	128	3	1	✓	✓	✓
ResBlock 4	Block4-1	128	3	1	✓	✓	✗
	Block4-2	128	3	1	✓	✓	✗
ResBlock 5	Block5-1	256	3	1	✓	✓	✓
	Block5-2	256	3	1	✓	✓	✓
ResBlock 6	Block6-1	256	3	1	✓	✓	✗
	Block6-2	256	3	1	✓	✓	✗
ResBlock 7	Block7-1	512	3	1	✓	✓	✓
	Block7-2	512	3	1	✓	✓	✓
ResBlock 8	Block8-1	512	3	1	✓	✓	✗
	Block8-2	512	3	1	✓	✓	✗
Classification		10	-	-	✗	✗	✗

Table 4: Hyperparameters for ResNet-18/CIFAR-10 on homogeneous clients

Datasets	#clients	#samples	distribution		augmentation
	100	500	i.i.d, non-i.i.d ( $\alpha = 1, 0.1$ )		flip, random crop
Training	#Rounds	#local epochs	batch size	#active clients	smooth factor $\kappa$
	1000	2	32	20	2.5
Optimization	Optimizer	Momentum	$wd$	initial $lr$	scheduler
	SGD	0.9	0.0005	0.1	cosine annealing